Inhibition of cyclooxygenase-2 in hematopoietic cells results in salt-sensitive hypertension

Ming-Zhi Zhang,[1,2] Bing Yao,[1] Yinqiu Wang,[1] Shilin Yang,[1] Suwan Wang,[1] Xiaofeng Fan,[1] and Raymond C. Harris[1,3,4]

[1]Department of Medicine, [2]Department of Cancer Biology, and [3]Department of Molecular Physiology and Biophysics, Vanderbilt University School of Medicine, Nashville, Tennessee, USA.

[4]Nashville Veterans Affairs Hospital, Nashville, Tennessee, USA.

Inhibition of prostaglandin (PG) production with either nonselective or selective inhibitors of cyclooxygenase-2 (COX-2) activity can induce or exacerbate salt-sensitive hypertension. This effect has been previously attributed to inhibition of intrinsic renal COX-2 activity and subsequent increase in sodium retention by the kidney. Here, we found that macrophages isolated from kidneys of high-salt–treated WT mice have increased levels of COX-2 and microsomal PGE synthase–1 (mPGES-1). Furthermore, BM transplantation (BMT) from either COX-2–deficient or mPGES-1–deficient mice into WT mice or macrophage-specific deletion of the PGE_2 type 4 (EP_4) receptor induced salt-sensitive hypertension and increased phosphorylation of the renal sodium chloride cotransporter (NCC). Kidneys from high-salt–treated WT mice transplanted with *Cox2*$^{-/-}$ BM had increased macrophage and T cell infiltration and increased M1- and Th1-associated markers and cytokines. Skin macrophages from high-salt–treated mice with either genetic or pharmacologic inhibition of the COX-2 pathway expressed decreased M2 markers and VEGF-C production and exhibited aberrant lymphangiogenesis. Together, these studies demonstrate that COX-2–derived PGE_2 in hematopoietic cells plays an important role in both kidney and skin in maintaining homeostasis in response to chronically increased dietary salt. Moreover, these results indicate that inhibiting COX-2 expression or activity in hematopoietic cells can result in a predisposition to salt-sensitive hypertension.

Introduction

There are more than 40 million people in the US alone with hypertension, and of these, the majority have salt-sensitive hypertension. In addition, at least a quarter of normotensive individuals also show salt sensitivity (1). Although the etiology of salt-sensitive hypertension is undoubtedly multifactorial, there is experimental and epidemiologic evidence linking abnormalities in the cyclooxygenase/prostaglandin (COX/PG) system to its pathogenesis. COX is the rate-limiting enzyme in metabolizing arachidonic acid to PGG_2 and subsequently to PGH_2, which serves as the precursor for subsequent metabolism by PG and thromboxane synthases. Prostanoid cellular responses are mediated by specific membrane–associated G-protein–coupled receptors. Receptor affinity for the prostanoids is in the nanomolar range, and prostanoids act locally on the tissues in which they are synthesized or on tissues adjacent to those in which they are formed. PGs are important mediators of many physiologic processes, including modulation of renal hemodynamics, salt and water handling, and renin production (2–8).

Two isoforms of COX exist in mammals, "constitutive" COX-1 and "inducible" COX-2. Both nonselective COX inhibitors (NSAIDs) and selective COX-2 inhibitors (coxibs) can elevate blood pressure (BP) and antagonize the BP-lowering effect of antihypertensive medication in many users (9). NSAIDs and COX-2 inhibitors can also induce peripheral edema (10, 11). A COX-2 polymorphism that reduces enzymatic activity has been associated with increased risk of stroke in African-Americans (12). Selective inhibition of COX-2 has also been implicated in increased cardiovascular mortality, which appears to be multifactorial and may involve increases in BP and salt and water retention in addition to accelerated thrombogenesis (13, 14).

The mechanism by which COX-2 inhibition leads to development or exacerbation of hypertension has been attributed to inhibition of intrinsic renal COX-2 activity, which leads to increased sodium retention by the kidney (9). However, recent studies have indicated an important role for immune cells in mediation and exacerbation of hypertension (15–17), with increased infiltration of both macrophages and lymphocytes in target organs (vasculature and kidney). In addition, studies by Titze and coworkers have shown that the skin is an important reservoir in the body for sodium, which is thought to interact with the negatively charged glycosoaminoglycan extracellular matrix (18). Skin macrophages appear to play an important role in preventing skin sodium accumulation, at least in part by promoting skin lymphangiogenesis, and macrophage depletion can predispose to development of salt-sensitive hypertension (19, 20). Macrophages express COX-2 and are a rich source of PGs, and macrophage-dependent COX-2 expression has been shown to be important for tumor- or inflammation-associated lymphangiogenesis (21). Therefore, in the current studies, we determined the role of COX-2–derived PG expression and activity in BM-derived cells in mediation of salt-sensitive hypertension.

▶ Related Commentary: p. 4008

Conflict of interest: Raymond C. Harris has consulted for Amgen, Lilly, Merck, and ProMetic.
Submitted: February 17, 2015; **Accepted:** September 3, 2015.
Reference information: *J Clin Invest*. 2015;125(11):4281–4294. doi:10.1172/JCI81550.

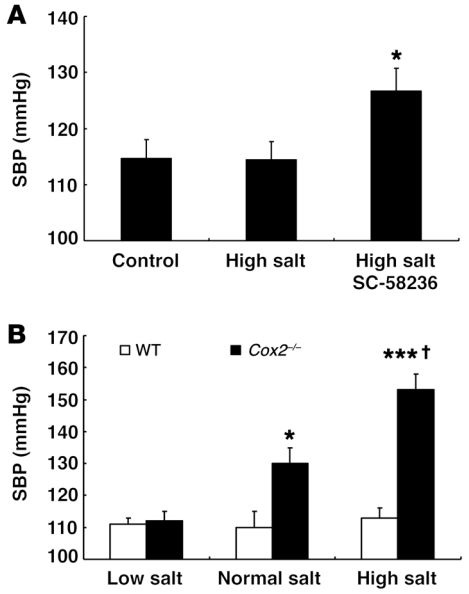

Figure 1. Genetic or pharmacologic COX-2 inhibition led to salt-sensitive hypertension. (**A**) SBP was elevated in mice (male, 129/SvJ) treated with a high-salt diet plus a selective COX-2 inhibitor, SC58236, but not in mice with a high-salt diet alone. *$P < 0.05$ vs. control and high-salt diet alone. $n = 4$ in each group. (**B**) WT and *Cox2*$^{-/-}$ mice (male, 2 months old, C57BL/6) were treated with a low-salt diet, normal-salt diet, or high-salt diet for 4 weeks, consecutively. SBP was similar between WT and *Cox2*$^{-/-}$ mice on a low-salt diet. Increasing dietary salt intake had no effect on SBP in WT mice, but led to progressive increases in SBP in *Cox2*$^{-/-}$ mice. *$P < 0.05$ vs. WT on a normal-salt diet; ***$P < 0.001$ vs. WT on a high-salt diet; $^{\dagger}P < 0.05$ vs. *Cox2*$^{-/-}$ on a normal-salt diet, $n = 5$ in each group. All values are shown as mean ± SEM. All P values were calculated by Student's t test.

Results

Global deletion of Cox2 led to salt-sensitive hypertension. Initial studies were performed in 129/SvJ mice, which are relatively resistant to the development of hypertension. However, these mice developed salt-sensitive hypertension when administered a high-salt diet plus the COX-2 inhibitor SC58236 (Figure 1A) and had increased renal macrophage infiltration (Supplemental Figure 1A; supplemental material available online with this article; doi:10.1172/JCI81550DS1). In C57BL/6 WT mice, BP was similar when the animals were fed a low-salt diet, a normal-salt diet, or a high-salt diet, consistent with the notion that C57BL/6 mice are resistant to development of salt-sensitive hypertension. In contrast, although C57BL/6 *Cox2*$^{-/-}$ mice had BPs similar to those of WT mice in response to a low-salt diet, they exhibited increased BP in response to a normal-salt diet (≈20 mmHg systolic BP [SBP]) and had further increases in BP in response to a high-salt diet (≈40 mmHg SBP) (Figure 1B). *Cox2*$^{-/-}$ mice also had increased renal macrophage infiltration (Supplemental Figure 1B). The increased salt sensitivity in the global *Cox2*$^{-/-}$ mice compared with WT mice treated with a COX-2 inhibitor may reflect more complete COX-2 inhibition as well as the well-described defects in postnatal nephrogenesis seen in global *Cox2*$^{-/-}$ mice (22, 23).

COX-2 expression and activity in BM-derived cells. Previous studies by us and others demonstrated that COX-2 is highly expressed in renal medullary interstitial cells and its expression is increased in response to high-salt intake. However, cells of monocytic lineage, tissue macrophages and dendritic cells, also reside in the renal interstitium and increase in response to hypertensive stimuli. Macrophages and dendritic cells are known to express high levels of COX-2. Therefore, we isolated renal macrophages/dendritic cells from WT mice on a high-salt diet using mouse CD11b microbeads, as we have previously described (24), and determined that they had increased mRNA levels of *Cox2* but not *Cox1* compared with mice on a normal-salt diet. There was also increased expression of microsomal PGE synthase–1 (*mPGES-1*), the enzyme primarily mediating PGE_2 synthesis from COX-2–derived PGH_2 (ref. 25 and Figure 2). In BM-derived cells from WT mice, PGE_2 was the predominant prostanoid produced (PGE_2: 101 ± 12; PGD_2: 60 ± 1; $PGF_{2\alpha}$: 14 ± 3; PGI_2: 0.92 ± 0.28; 11δ-TXB_2: 0.26 ± 0.01 ng/mg protein). Of note, in BM-derived cells from *Cox2*$^{-/-}$ mice, the major decrease in prostanoids resulted from decreased PGE_2 production (PGE_2: 69 ± 3 [$P < 0.05$]; PGD_2: 62 ± 14; $PGF_{2\alpha}$: 13 ± 3; PGI_2: 0.24 ± 0.03 [$P < 0.05$]; 11δ-TXB_2: 0.26 ± 0.03 ng/mg protein; $n = 3$ in each group).

Hematopoietic COX-2 deficiency increased BP in response to chronic high-salt exposure. In order to investigate the role of immune cells in COX-2–mediated regulation of BP, BM transplantation (BMT) was performed from either WT or *Cox2*$^{-/-}$ males into syngeneic animals. In initial studies, BM from males was transplanted into females in order to assess effective engraftment. In all subsequent studies, male BM was transplanted into males, and all BP studies were therefore performed on male animals. In animals on a normal-salt diet, there were no differences in serum electrolytes or hematocrit (Supplemental Table 1).

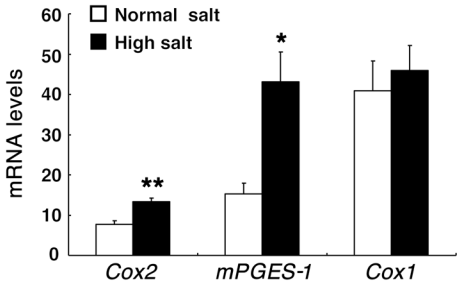

Figure 2. Renal macrophage/dendritic cell mRNA levels of *Cox2* and *mPGES-1* were increased in response to high-salt intake. Male C57BL/6 mice (2 months old) were treated with a normal-salt diet (control) or high-salt diet for 4 weeks, and renal macrophages/dendritic cells were isolated with CD11b microbeads. *$P < 0.05$; **$P < 0.01$. $n = 5$ in each group. All values are shown as mean ± SEM. All P values were calculated by Student's t test.

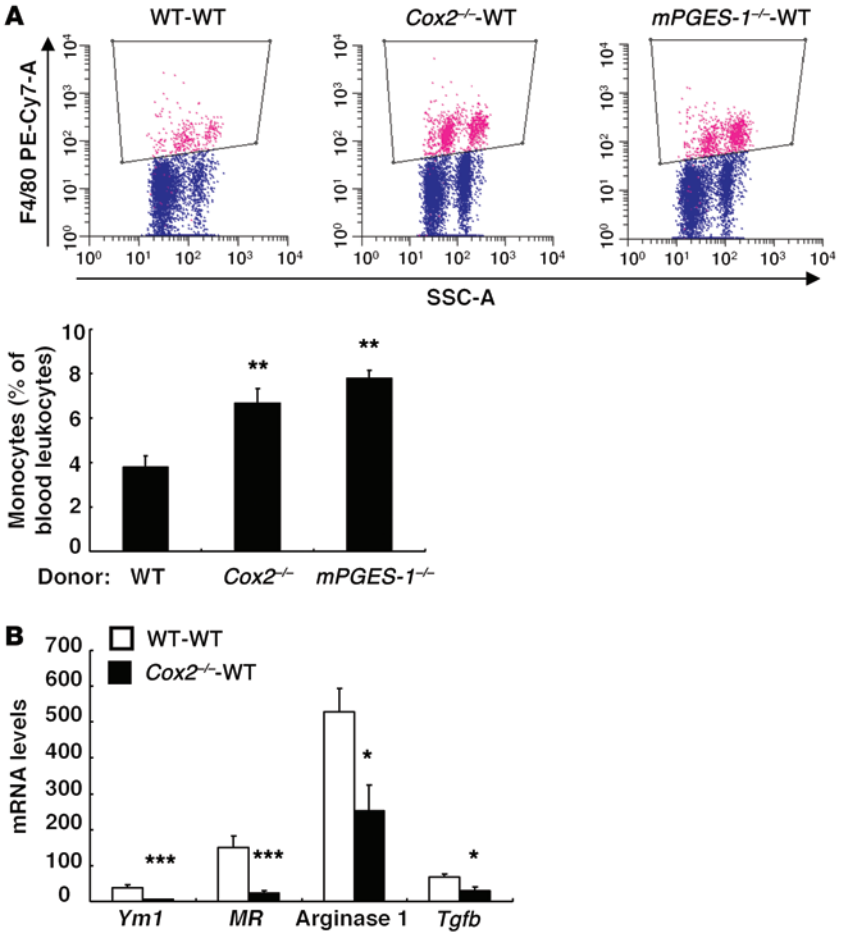

Figure 3. COX-2 expression modulated monocyte and peritoneal macrophage responses to high-salt intake. (**A**) Flow cytometric analysis determined that blood monocyte density was higher in *Cox2*$^{-/-}$-WT BMT and *mPGES-1*$^{-/-}$-WT BMT mice than in WT-WT BMT mice in response to a high-salt diet. $^{**}P < 0.01$ vs. high-salt diet–treated WT-WT BMT mice. $n = 5$. (**B**) Peritoneal macrophages from high-salt diet–treated *Cox2*$^{-/-}$-WT BMT mice had reduced mRNA levels of M2 markers, *Ym1*, *MR*, arginase-1, and *Tgfb*. $^{*}P < 0.05$; $^{***}P < 0.001$ vs. high-salt diet–treated WT-WT BMT mice. $n = 5$ in each group. All values are shown as mean ± SEM. All *P* values were calculated by Student's *t* test.

A high-salt diet increased the percentage of monocytes in blood of *Cox2*$^{-/-}$-WT BMT mice compared with WT-WT BMT mice (Figure 3A). However, peritoneal macrophages isolated from *Cox2*$^{-/-}$-WT BMT mice had decreased mRNA expression of anti-inflammatory and reparative ("M2") phenotypic markers (*Ym1*, arginase-1, mannose receptor [*MR*, *Cd206*], *Tgfb*) (Figure 3B). Kidneys from *Cox2*$^{-/-}$-WT BMT mice treated with high salt had increased expression of the pan–T cell marker CD3 and the macrophage marker F4/80, but had decreased expression of a marker of Tregs, forkhead box P3 (FOXP3) (Figure 4A). High-salt–treated *Cox2*$^{-/-}$-WT BMT kidneys also had decreased expression of the macrophage M2 markers MR (Figure 4, B and C) and arginase-1 (Figure 4D), but increased expression of the M1 marker iNOS (Figure 4A) and increased mRNA expression of M1/Th1 markers/cytokines (*Inos*, *Ccl3*, *Tnfa*, *Il1a*, *Il1b*) (Figure 4E). Treatment with the COX-2 inhibitor SC58236 also resulted in decreased expression of macrophage M2 markers and increased iNOS and Th1 cytokines in kidneys from WT mice on a high-salt diet (Supplemental Figure 2A). Furthermore, freshly isolated peritoneal macrophages incubated with SC58236 for 24 hours had decreased expression of the M2 markers (MR, arginase-1) and increased expression of the proinflammatory ("M1") marker TNF-α (Supplemental Figure 2B).

When mice (on either a C57BL/6 or a 129/SvJ background) were maintained on a regular diet, there were no BP differences noted between WT-WT BMT mice and *Cox2*$^{-/-}$-WT BMT mice. However, when placed on a high-salt diet for 4 to 6 weeks, there was a significant increase in BP in *Cox2*$^{-/-}$-WT BMT mice compared with WT-WT BMT mice (10 to 15 mmHg, $n = 6$–8) (Figure 5A), in association with increased heart hypertrophy (heart weight/body weight ratios: 0.00466 ± 0.00013 vs. 0.00388 ± 0.00017; $P < 0.01$, $n = 4$) (Supplemental Figure 3A), suggesting that the hematopoietic cell COX-2 plays an important role in maintenance of BP in response to chronic high-salt intake. As validation, we also monitored BP in high-salt–treated WT-WT and *Cox2*$^{-/-}$-WT mice with radiotelemetry and found significantly increased BP in the mice with *Cox2* deletion in their hematopoietic cells (Figure 5B). However, we saw no differences in urinary PGE-M excretion (17.16 ± 1.56 vs. 15.74 ± 2.35 ng/mg creatinine of WT-WT BMT, $n = 4$).

Salt-sensitive hypertension was also noted in mice with BMT from mice with deletion of *mPGES-1* (*mPGES-1*$^{-/-}$-WT BMT) (Figure 6A). WT-WT BMT mice on a high-salt diet significantly increased BP when treated with SC58236, but there was no further increase with COX-2 inhibitor treatment of *Cox2*$^{-/-}$-WT BMT mice (Figure 6B). When BM from *Cox2*$^{-/-}$ mice was transplanted into global *Cox2*$^{-/-}$ mice, they continued to demonstrate salt-sensitive hypertension, but when BM from WT mice was transplanted into *Cox2*$^{-/-}$ mice, there was partial amelioration of salt-sensitive hypertension (Figure 6C).

Deletion of EP$_4$ *in macrophages increased BP in response to chronic high-salt exposure*. The PGE_2 type 4 (EP_4) receptor is the most highly expressed PGE_2 receptor subtype in macrophages, with lower expression levels of other PGE_2 receptor subtypes, EP_2 and EP_3 (26). We confirmed EP_4 expression in the mouse macrophage cell line RAW 264.7 (Supplemental Figure 4A) and found that administration of a selective EP_4 inhibitor, L-161,982, increased expression of M1 markers (Supplemental Figure 4B), while administration of PGE_2 decreased expression of *Inos* mRNA, which was reversed by simultaneous treatment with L-161,982 (Supplemental Figure 4C). We generated mice with selective monocyte/macrophage/dendritic EP_4 deletion by crossing *EP4*$^{fl/fl}$ mice with *Cd11b-Cre* mice, all on a C57BL/6 background, and confirmed effective deletion in peritoneal macrophages from the *Cd11b-Cre EP4*$^{fl/fl}$ mice (Supplemental Figure 5). Similarly to the mice with either global or selective hematopoietic deletion of Cox2, *Cd11b-*

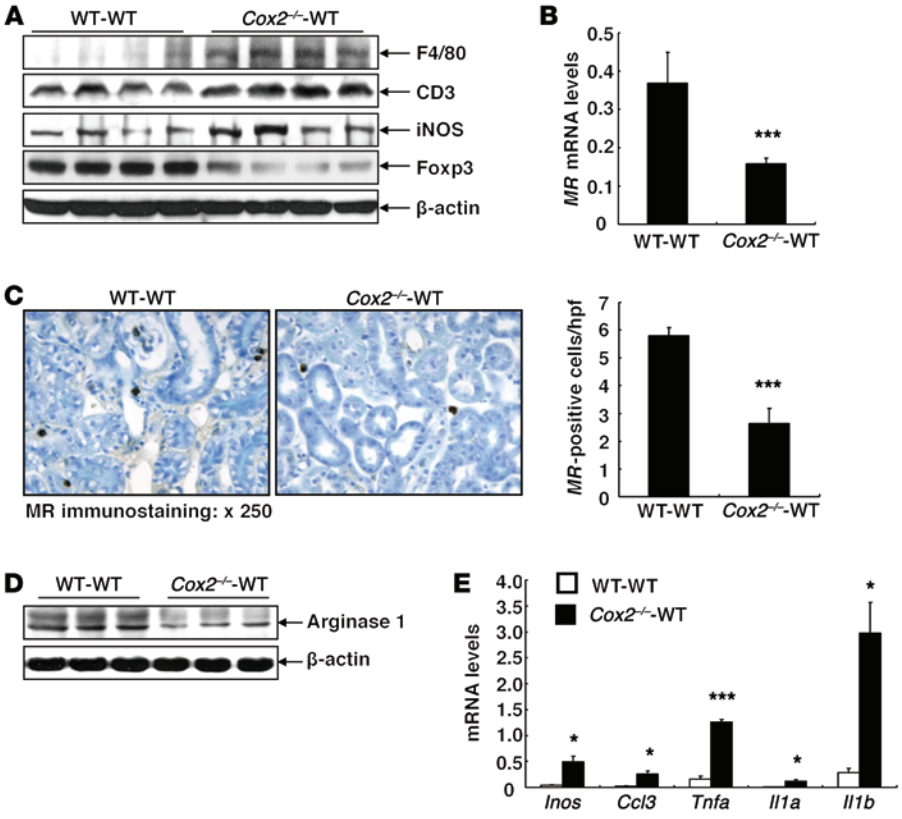

Figure 4. Kidneys from mice with hematopoietic cell COX-2 deficiency had higher levels of Th1 cytokines and exhibited M1 phenotypic macrophages/dendritic cells in response to high-salt intake. (**A**) Immunoblotting demonstrated that high-salt diet–treated *Cox2*$^{-/-}$-WT BMT mouse kidneys had increased protein levels of F4/80 (a marker of macrophages/dendritic cells), CD3 (a marker of T cells), and iNOS (a marker of M1 phenotype), but decreased protein levels of a Treg marker, FOXP3. (**B**–**D**) High-salt diet–treated *Cox2*$^{-/-}$-WT BMT mouse kidneys had decreased mRNA levels (**B**) and decreased immunoreactivity (**C**) of *MR* as well as decreased protein levels of arginase-1, markers of an M2 phenotypic macrophages/dendritic cells (**D**). ***$P < 0.001$ vs. high-salt diet–treated WT-WT BMT mice. $n = 4$ in each group. Original magnification, ×250. (**E**) High-salt diet–treated *Cox2*$^{-/-}$-WT BMT mouse kidneys had increased mRNA levels of M1/Th1 markers/cytokines *Inos*, *Ccl3*, *Tnfa*, *Il1a*, and *Il1b*. *$P < 0.05$; ***$P < 0.001$ vs. high-salt diet–treated WT-WT BMT mouse kidneys. $n = 4$ in each group. All values are shown as mean ± SEM. All *P* values were calculated by Student's *t* test.

Cre EP4$^{fl/fl}$ mice demonstrated salt-sensitive hypertension (Figure 7A) and had increased heart weight/body weight ratios (*Cd11b-Cre EP4*$^{fl/fl}$ vs. *EP4*$^{fl/fl}$: 0.00581 ± 0.00007 vs. 0.00476 ± 0.00020; $P < 0.001$, $n = 4$) (Supplemental Figure 3B). The kidneys of *Cd11b-Cre EP4*$^{fl/fl}$ mice also exhibited increased expression of the pan–T cell marker CD3, the effector T cell marker CD8, the neutrophil marker Ly-6G, and the macrophage marker F4/80 (Figure 7B), but decreased expression of M2 markers (Figure 7C).

Of note, in kidneys from both *Cox2*$^{-/-}$-WT BMT and *mPGES-1*$^{-/-}$-WT BMT mice on a high-salt diet, there was increased sodium chloride cotransporter (*NCC*) mRNA expression (Figure 8A). There was also increased NCC phosphorylation at threonine and serine residue targets of SPAK and OSR1 (ref. 27, Figure 8B, and Supplemental Figure 6). In addition, there was increased renal expression of serum/glucocorticoid-regulated kinase 1 (SGK-1) (Figure 8, C and D) and increased cortical colocalization of SGK-1 and phosphorylated NCC (p-NCC) (Figure 8D).

Deletion of hematopoietic cell Cox2 impaired skin lymphangiogenesis in response to high salt. Previous studies by Titze and colleagues indicated that increased salt deposition in the skin is associated with hypertension (28), which is normally prevented by skin macrophages that respond to alterations in osmolarity by nuclear factor of activated T cells 5–dependent (NFAT5-dependent) (tonicity enhancer binding protein [TonEBP]) transcription of VEGF-C, thereby mediating skin lymphangiogenesis via VEGFR-3 (19). In the present studies, we also found that, compared with skin from mice on a normal-salt diet, the skin of WT mice on a high-salt diet had increased mRNA expression of *Vegfc* and the lymphatic marker podoplanin. Of note, simultaneous administration of SC58236 inhibited this increased expression (Figure 9).

RAW 264.7 cells were cultured with or without LPS to polarize to an M1 phenotype or IL-4/IL-13 to polarize to an M2 phenotype. They were then incubated for 5 hours with or without the addition of 40 mm NaCl, a maneuver recently shown to induce a Th17 phenotype in naive CD4$^+$ T cells (29, 30). In all 3 phenotypic subtypes, increased medium NaCl markedly increased *Cox2* mRNA expression, with the greatest proportional increase seen in M2 macrophages. Furthermore, the NaCl-treated macrophages all had increased expression of *Nfat5* and *Vegfc* mRNA (Figure 10). Increased medium NaCl led to upregulation of *Cox2* and *Nfat5* expression by 2.5 hours, while *Vegfc* was only increased at 5 hours (Supplemental Figure 7A). PGE_2 administration increased *mPGES-1*$^{-/-}$ expression in isolated peritoneal macrophages from WT mice (Supplemental Figure 7B).

In preliminary studies, we determined skin sodium content in ashed skin (19) and found a marked, 20%–25%, increase in the skin from *Cox2*$^{-/-}$-*Cox2*$^{-/-}$ BMT mice compared with WT-WT BMT mice fed a high-salt diet (Supplemental Figure 8A). We also found increased skin water content (Supplemental Figure 8B). Skin from WT-WT BMT mice had increased *Cox2* expression on a high-salt diet compared with normal diet (relative *Cox2* mRNA levels: 0.152 ± 0.024 vs. 0.062 ± 0.010; $P < 0.05$, $n = 4$). Skin macrophages from high-salt–treated WT-WT BMT mice expressed COX-2 (Figure 11A). Compared with high-salt–treated WT-WT BMT mice, skin macrophages from high-salt–treated *Cox2*$^{-/-}$-WT BMT mice also had markedly decreased expression of VEGF-C (Figure 11B). High-salt–treated *Cox2*$^{-/-}$-WT BMT mice had increased macrophages in skin compared with those of WT-WT BMT mice, but the *Cox2*$^{-/-}$-WT BMT macrophages had decreased expression of the M2 marker MR (Fig-

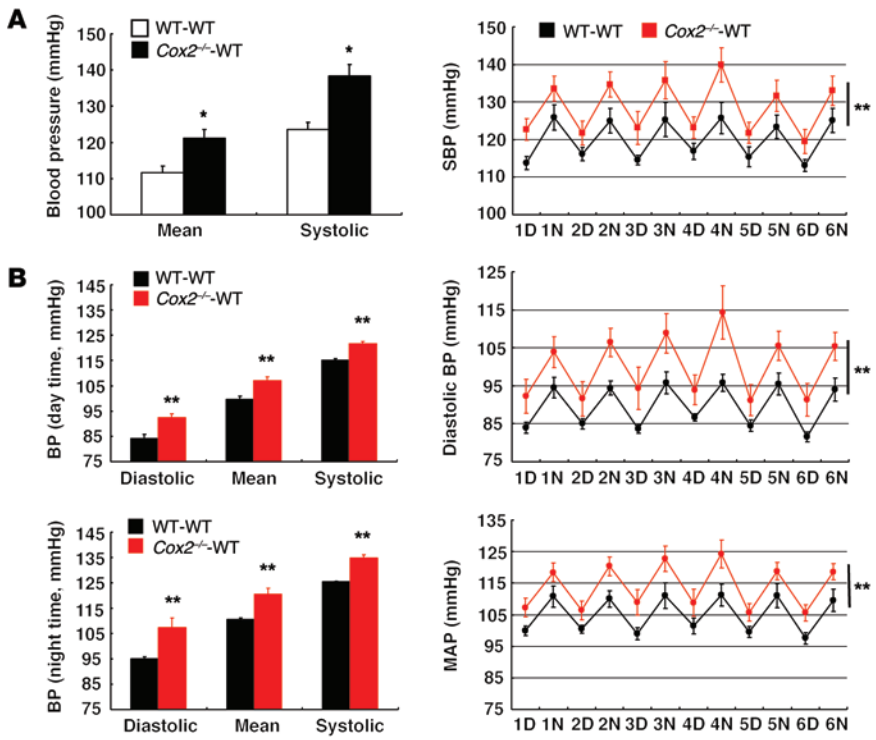

Figure 5. Mice with hematopoietic cell COX-2 deficiency developed salt-sensitive hypertension. Six weeks after BMT, mice were treated with high-salt diet for 4 to 6 weeks and BP was measured in conscious animals using carotid catheterization (**A**) or radiotelemetry (**B**). (**A**) Both mean arterial pressure (MAP) and SBP were higher in high-salt diet–treated *Cox2*$^{-/-}$-WT BMT than in their corresponding high-salt diet–treated WT-WT BMT controls. **P* < 0.05 vs. high-salt diet–treated WT-WT BMT mice. *n* = 6 in each group. All values are shown as mean ± SEM. All *P* values were calculated by Student's *t* test. (**B**) BP was monitored with radiotelemetry 14 days after transmitter implantation. D, day; N, night. Data are expressed as mean ± SEM. *n* = 5 per group. Data were analyzed by repeated measures, 2-way ANOVA and Student's *t* test. ***P* < 0.01.

ure 12A). There were similar increases and altered polarization of skin macrophages in *Cd11b-Cre EP4*$^{fl/fl}$ and SC58236-treated *EP4*$^{fl/fl}$ mice on a high-salt diet (Figure 12B).

The skin of *Cox2*$^{-/-}$-WT BMT mice on a high-salt diet exhibited abnormal lymphangiogenesis, as indicated by a decreased number of lymphatic ducts detected by the lymphatic markers LYVE and podoplanin (Figure 13, A and B). In addition, the skin lymphatic ducts observed in the *Cox2*$^{-/-}$-WT BMT mice were markedly dilated compared with those of WT-WT BMT mice (Figure 13C). Similar decreased skin lymphatic ducts and increased ductal dilation were also observed in high-salt–treated *Cd11b-Cre EP4*$^{fl/fl}$ mice and in high-salt plus SC58236–treated *EP4*$^{fl/fl}$ mice (Figure 13, D–F).

As a functional measure of lymphatic function, tail lymphatic flow was measured by injecting a large (2,000 kDa) FITC-labeled dextran that is taken up by lymphatics but not capillaries (31, 32). Lymphatic flow was markedly decreased in high-salt–treated *Cox2*$^{-/-}$-WT BMT mice compared with high-salt–treated WT-WT BMT mice (Figure 14A). *Cd11b-Cre EP4*$^{fl/fl}$ mice also had marked decreases in lymphatic flow rates compared with *EP4*$^{fl/fl}$ mice on a high-salt diet. Furthermore, chronic administration of SC58236 to high-salt–treated *EP4*$^{fl/fl}$ mice also led to decreased tail lymphatic flow (Figure 14B).

Discussion

COX-2 inhibitors, as well as nonselective NSAIDs, can elevate BP and exacerbate existing hypertension to an extent that may potentially increase hypertension-related morbidity (9, 33). NSAIDs and COX-2 inhibitors have also been reported to induce peripheral edema in up to 5% of the general population (10, 11). The mechanism by which COX-2 inhibition leads to development or exacerbation of salt-sensitive hypertension has been generally posited to be due primarily to inhibition of intrinsic renal COX-2 activity, since salt loading upregulates COX-2 expression in renal medulla (34, 35) and COX-2 inhibitors reduce urinary sodium excretion during the initial period of treatment when sodium loaded (36–40). In addition to intrarenal COX-2, the current studies indicated that with chronic salt loading, COX-2–generated PGs from BM-derived cells mediate BP homeostasis such that selective deletion of either COX-2 expression (*Cox2*$^{-/-}$-WT BMT) or PGE_2 production (*mPGES-1*$^{-/-}$-WT BMT) in these cells predisposed to salt-sensitive hypertension. Furthermore, selective deletion of the PGE_2 receptor subtype EP_4 in monocytes/macrophages also led to development of salt-sensitive hypertension.

The mechanism by which deletion of PGE_2 production or signaling in hematopoietic cells leads to development of hypertension appears to be multifactorial. BM-derived cells are known to be a rich source of PGs, and cells of monocytic origin express high levels of COX-2. Myeloid cell COX-2–derived PGE_2 is implicated in colonic tumorigenesis (41), and macrophage-derived PGE_2 is essential for promoting the M2/Th2 phenotype seen in infiltrating cells in tumors (42), an effect that is mediated by EP_4 activation. EP_4 is the predominant PG receptor in macrophages (26), and EP_4 activation in macrophages inhibits macrophage cytokine and chemokine release (43). In the current studies, lack of COX-2 or inhibition of EP_4 signaling altered macrophage/dendritic cell polarization, leading to a proinflammatory or M1-like phenotype rather than an M2-like phenotype; these findings are consistent with previous studies (21, 43). The net effect was a relative increase in macrophages as well as T cells and neutrophils in the kidney, which may then promote a proinflammatory phenotype.

Macrophage infiltration of the kidney is a consistent finding in experimental models of hypertension (44). Decreased macrophage infiltration has been associated with amelioration of hypertension in some (45–47), but not all studies (48, 49). It has been

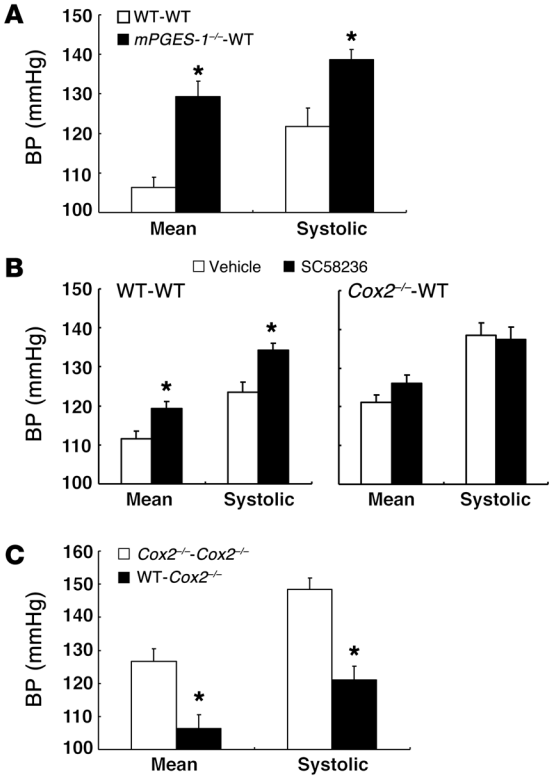

Figure 6. Mice with deficiency of hematopoietic cell COX-2 pathway developed salt-sensitive hypertension. Six weeks after BMT, mice were treated with high-salt diet for 4 to 6 weeks and BP was measured in conscious animals using carotid catheterization. (**A**) Both mean arterial pressure and SBP were higher in high-salt diet–treated *mPGES-1*$^{-/-}$-WT BMT mice than in high-salt diet–treated WT-WT BMT controls. *$P < 0.05$ vs. high-salt diet–treated WT-WT BMT mice. $n = 6$ in each group. (**B**) Treatment with a selective COX-2 inhibitor, SC58236, increased both mean arterial pressure and SBP in high-salt diet–treated WT-WT BMT mice, but not in high-salt diet–treated *Cox2*$^{-/-}$-WT BMT mice. *$P < 0.05$ vs. vehicle group. $n = 6$ in vehicle group; $n = 4$ in SC58236 group. (**C**) Both mean arterial pressure and SBP were higher in high-salt diet–treated *Cox2*$^{-/-}$-*Cox2*$^{-/-}$ BMT mice than in high-salt diet–treated WT-*Cox2*$^{-/-}$ BMT mice.*$P < 0.05$ vs. high-salt diet–treated *Cox2*$^{-/-}$-*Cox2*$^{-/-}$ BMT mice. $n = 4$ in each group. All values are shown as mean ± SEM. All *P* values were calculated by Student's *t* test.

suggested that the lack of improvement in the latter studies may be due to global deletion of all macrophages, both proinflammatory (M1) and antiinflammatory (M2) phenotypes (44).

Recent studies have indicated an important role for T cells in development of hypertension (reviewed in refs. 44 and 50) and have also indicated an important role for dendritic cell activation of T cells in this mediation of hypertension (51). COX-2–derived PGs from dendritic cells can suppress T cell activation (52). PGE_2 can act directly on T cells, including CD4, CD8, and Th17 subtypes. PGE_2 suppresses CD4 Th cell differentiation to a Th1 phenotype (53), and PGE_2 reduces production of Th1 cytokines such as IFN-γ and IL-2, blocks cell-surface expression of cytokine receptors, and directly inhibits CD8 T cell proliferation and differentiation (54). In addition, both T cells and B cells can themselves express COX-2 (55, 56).

In the current studies, it was also noteworthy that both NCC expression and phosphorylation were increased in the kidneys of mice with alterations in macrophage/dendritic cell COX-2 expression or activity, since NCC phosphorylation indicates increased activation of the transporter (57). In preliminary studies, we also noted increased expression of epithelial sodium channel (*ENaC*) mRNA in high-salt–treated *Cox2*$^{-/-}$-WT BMT and *mPGES*$^{-/-}$-WT BMT mice (Supplemental Figure 9). Previous studies have indicated activation of distal sodium transporters in angiotensin-mediated hypertension, an effect proposed to be due at least in part to T cell activation (58, 59). Of note, previous studies by Jia et al. in global *mPGES* knockout mice reported relative increases in expression of NCC and ENaC in response to aldosterone-induced hypertension (60). There have not been previous studies indicating a role for PGs in direct regulation of NCC, and in the current studies, we did not determine whether the observed NCC phosphorylation was a direct effect of decreased PGE_2 or was mediated by other cytokines or factors released by macrophages or T cells. To confirm that the effects of hematopoietic COX-2 inhibition did

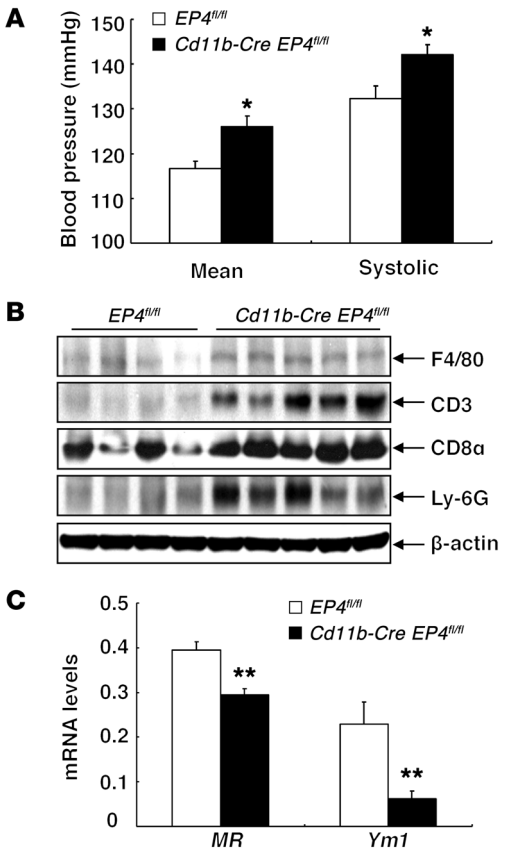

Figure 7. Mice with macrophage *EP4* receptor deletion developed salt-sensitive hypertension. (**A**) BP was higher in high-salt diet–treated *Cd11b-Cre EP4*$^{fl/fl}$ mice than in age-matched high-salt diet–treated *EP4*$^{fl/fl}$ mice. *$P < 0.05$. $n = 4$ in each group. (**B**) Immunoblotting demonstrated that high-salt diet–treated *Cd11b-Cre EP4*$^{fl/fl}$ mouse kidneys had increased protein expression levels of F4/80, CD3, CD8α (an indicator of cytotoxic T cells), and Ly-6G (a marker of neutrophils). (**C**) The mRNA levels of M2 markers *MR* and *Ym1* were lower in high-salt diet–treated *Cd11b-Cre EP4*$^{fl/fl}$ mouse kidney than in high-salt diet–treated *EP4*$^{fl/fl}$ mouse kidney. **$P < 0.01$. $n = 6$ in each group. All values are shown as mean ± SEM. All *P* values were calculated by Student's *t* test.

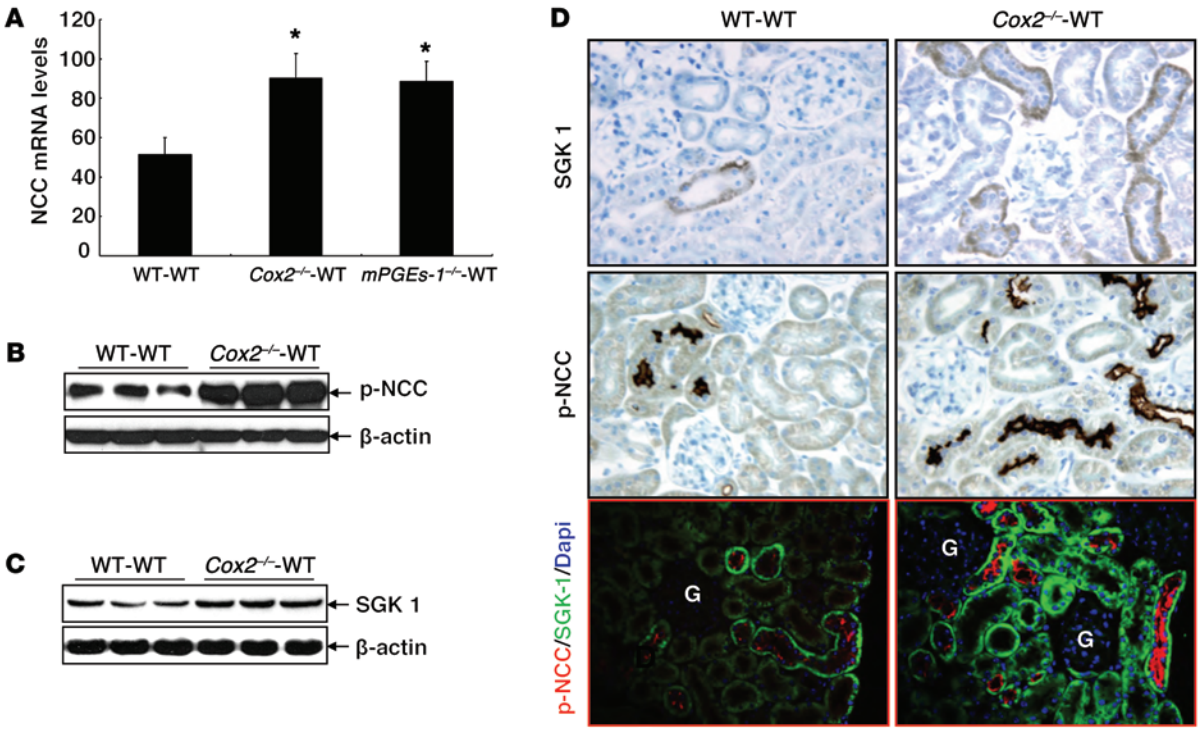

Figure 8. Renal NCC activity was increased in high-salt diet–treated mice with inhibition of hematopoietic cell COX-2 pathway. (**A**) *NCC* mRNA levels were higher in high-salt diet–treated *Cox2*$^{-/-}$-WT BMT and *mPGES-1*$^{-/-}$-WT BMT mice than in high-salt diet–treated WT-WT BMT controls. **P* < 0.05. *n* = 6 in each group. All values are shown as mean ± SEM. All *P* values were calculated by Student's *t* test. (**B**–**D**) Both renal NCC activity (p-NCC) and SGK-1 expression were higher in high-salt diet–treated *Cox2*$^{-/-}$-WT BMT than in high-salt diet–treated WT-WT BMT controls and were colocalized in distal convoluted tubule in renal cortex. G, glomerulus. Original magnification, ×250. Note: the samples in **C** are identical to those used for Figure 4D, so the same β-actin control was utilized.

not mediate renal responses to an acute salt load, we evaluated sodium and water balance with acute salt loading in *Cox2*$^{-/-}$-WT and *CD-11b-Cre EP4*$^{fl/fl}$ mice and found no difference from control mice on sodium and water homeostasis (Supplemental Figure 10).

In addition to potential alterations of renal function, disruption of hematopoietic COX-2 expression or signaling also led to alterations in skin lymphangiogenesis. Titze and coworkers found that skin macrophages sense alterations in skin interstitial electrolyte accumulation and thereby increase local lymphangiogenesis via increased expression of the transcription factor, TonEBP (NFAT5), which is implicated in increased expression of the lymphangiogenesis promoter VEGF-C (19, 20). Macrophage depletion or inhibition of TonEBP decreased skin VEGF-C levels, inhibited skin lymphangiogenesis, and led to development of salt-sensitive hypertension (19, 20, 61).

Previous studies have demonstrated an important role for M2 macrophages and macrophage COX-2–derived PGs in lymphangiogenesis associated with tumors, inflammation, or secondary lymphedema via increased VEGF-C expression (62–66). The present studies demonstrate that treatment with a COX-2 inhibitor inhibited high-salt–mediated increases in skin VEGF-C expression, and skin macrophages from high-salt–treated *Cox2*$^{-/-}$-WT BMT mice had decreased VEGF-C expression. Furthermore, incubating cultured macrophages with 40 mM additional NaCl increased mRNA expression for *Cox2* as well as *Nfat5* and *Vegfc*. In this regard, previous studies by Wiig et al. indicated that, with salt accumulation in the skin, there was substantially higher sodium concentration in the skin lymphatic fluid compared with plasma (61). In addition, there was a marked decrease in lymphangiogenesis in the skin of high-salt–treated mice with

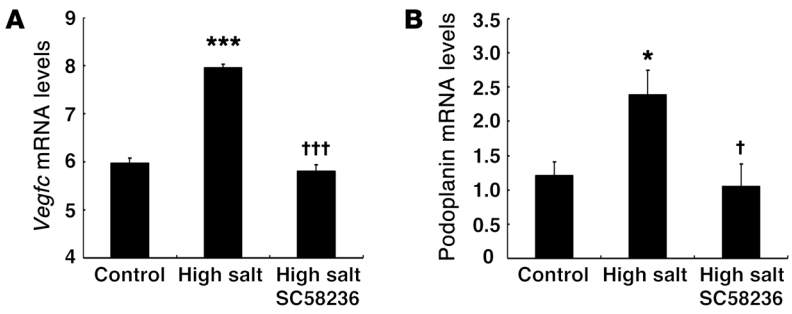

Figure 9. COX-2 contributed to skin lymphangiogenesis induced by high-salt intake. Male WT mice were treated with a high-salt diet for 4 weeks, and ear skin was harvested for qPCR. High-salt diet–induced increases in skin mRNA levels of *Vegfc* (**A**) and podoplanin (**B**) were abolished by treatment with a selective COX-2 inhibitor, SC58236. **P* < 0.05, ****P* < 0.001 vs. control group; †*P* < 0.05, †††*P* < 0.001 vs. high-salt–treated group. *n* = 4 in each group. All values are shown as mean ± SEM. All *P* values were calculated by ANOVA and Bonferroni's *t* test.

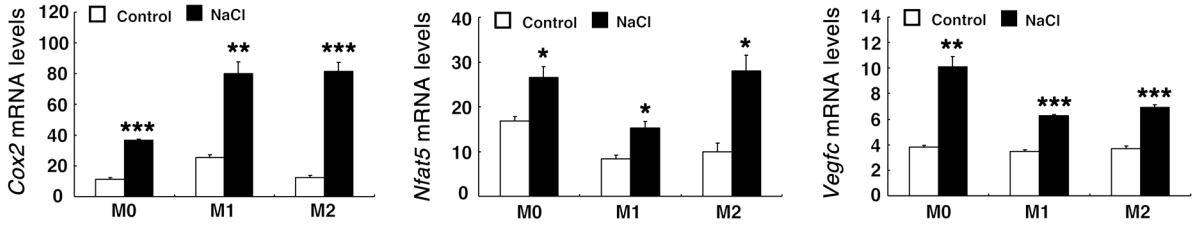

Figure 10. Increases in medium NaCl led to elevated mRNA levels of *Cox2* and *Nfat5* and *Vegfc* in cultured murine macrophage RAW 264.7 cells. RAW 264.7 cells were cultured with or without the M1 inducer LPS or the M2 inducers IL-4/IL-13 and then incubated for 5 hours in medium with or without addition of 40 mM NaCl. Increased medium NaCl concentration elevated mRNA levels of *Cox2*, *Nfat5*, and *Vegfc* in all phenotypes. $^{*}P < 0.05$; $^{**}P < 0.01$; $^{***}P < 0.001$ vs. controls. $n = 3$ in each group. All values are shown as mean ± SEM. All *P* values were calculated by Student's *t* test.

Cox2 deletion in hematopoietic cells or with EP_4 receptor deletion in macrophages as well as pharmacologic COX-2 inhibition in association with decreased lymphatic flow. Further studies will be required to determine the relative importance of alterations in skin versus kidney responses to chronic salt loading when hematopoietic COX-2 is inhibited.

In summary, these studies suggest that COX-2–derived PGE_2 in hematopoietic cells plays an important role in both kidney and skin in maintaining homeostasis in response to chronically increased dietary salt and that inhibiting COX-2 expression or activity in these cells can predispose to salt-sensitive hypertension.

Methods

Animal studies. *Cox2*$^{-/-}$ mice on a 129/BL6 background were originally generated by Dinchuk et al. (67). Heterozygous breeding pairs were obtained from Jackson Laboratory (stock 002476) and backcrossed onto a C57BL/6 background or a 129/SvJ background for 12 generations. Homozygous C57BL/6 *mPGES-1*$^{-/-}$ mice as BM donors were also purchased from Jackson Laboratory (stock 009135). *EP4*$^{fl/fl}$ mice were generated in M. Breyer's laboratory (68), and *CD11b-Cre* mice with transgene integration in the Y chromosome were generated in J. Vacher's laboratory (69); both types of mice were on a C57BL/6 background. Mice were crossed to generate *EP4*$^{fl/fl}$ mice (WT control) and *Cd11b-Cre EP4*$^{fl/fl}$ mice (mice with macrophage and dendritic cell *EP4* deletion). For experiments with alterations of dietary salt intake, mice were given a low-salt diet (0.02% to 0.03% NaCl, ICN Biochemicals) for 4 weeks or a normal-salt diet (1% NaCl, LabDiet) or a high-salt diet (8% NaCl, Research Diets) for 4 to 6 weeks. The COX-2 inhibitor SC58236 (a gift from Searle Monsanto) was given at a dose of 2 mg/kg by daily gastric gavage. Unless otherwise indicated, the mice were maintained on a normal chow diet.

Creation of chimeric mice. BMT was performed as previously described (70). Briefly, recipient mice were lethally irradiated with 9 Gy using a cesium γ source. BM cells were harvested from the donor femurs and tibias. Recipient mice received 5×10^6 BM cells in 0.2 ml medium through tail-vein injection. Five weeks after transplantation,

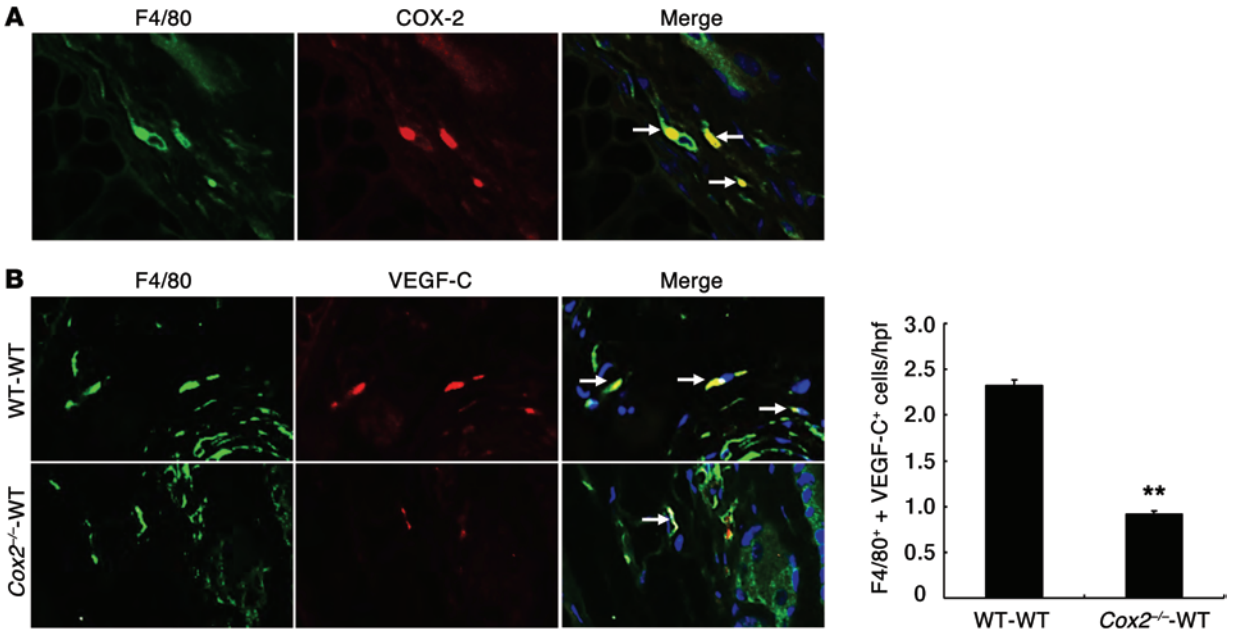

Figure 11. COX-2 influenced skin macrophage VEGF-C expression to high-salt intake. (**A**) Skin macrophages from high-salt diet–treated WT-WT BMT mice expressed COX-2. (**B**) High-salt diet–treated *Cox2*$^{-/-}$-WT BMT mice had decreased skin VEGF-C–expressing macrophages compared with high-salt diet–treated WT-WT BMT mice. $^{**}P < 0.01$. $n = 4$. Arrows indicate cells expressing both F4/80 and COX-2 (**A**), or both F4/80 and VEGF-C (**B**). Original magnification, ×400. All values are shown as mean ± SEM. All *P* values were calculated by Student's *t* test.

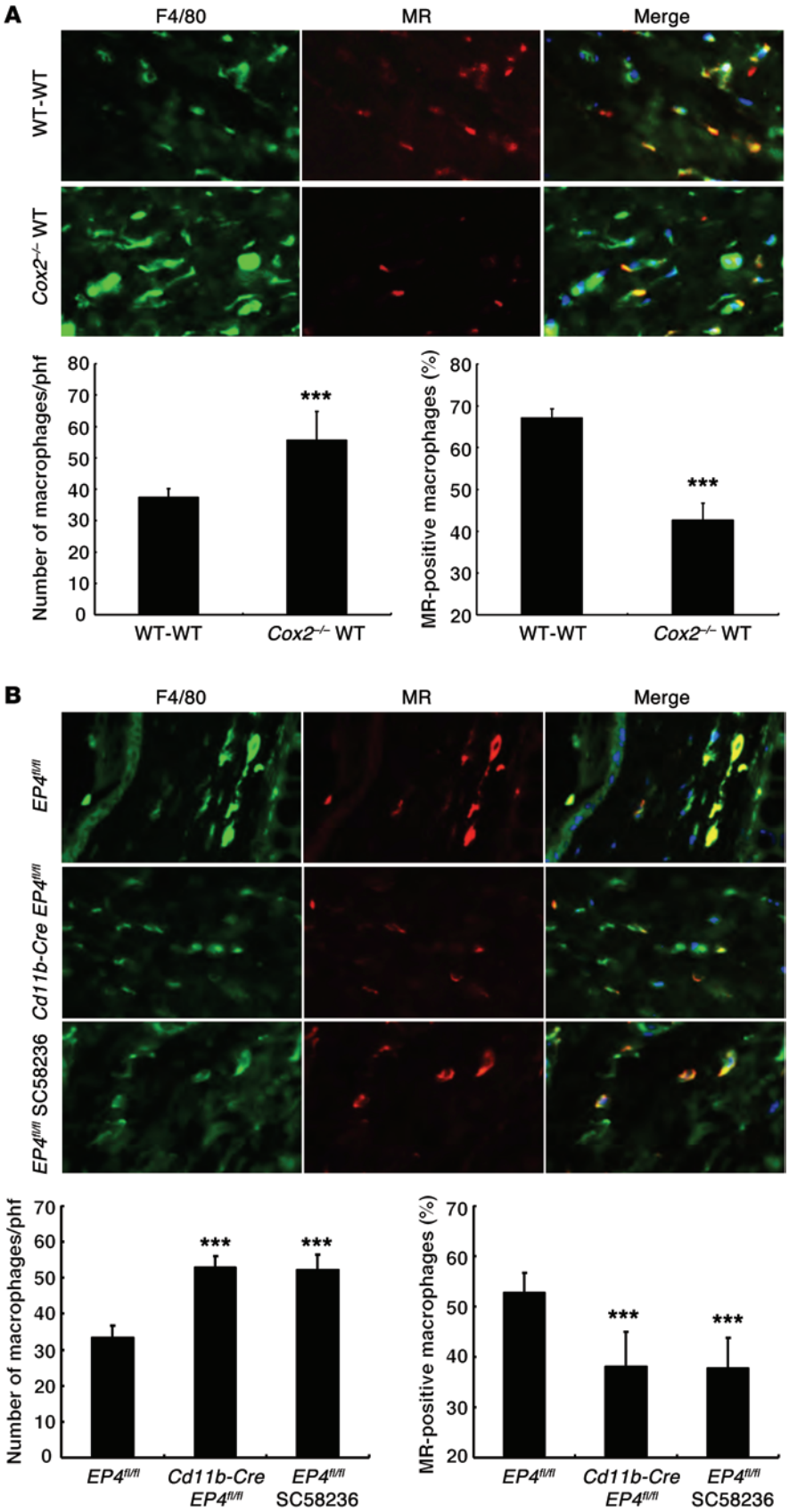

Figure 12. COX-2 expression influenced phenotypic and functional responses of skin macrophages to high-salt intake. (**A**) High-salt diet–treated *Cox2*$^{-/-}$-WT BMT mice had increased total skin macrophages, but decreased M2 macrophages compared with high-salt diet–treated WT-WT BMT mice. ***$P < 0.001$. $n = 4$. (**B**) Both high-salt diet–treated *Cd11b-Cre EP4*$^{fl/fl}$ and high-salt diet plus SC58236–treated *EP4*$^{fl/fl}$ mice had increased total skin macrophages, but decreased M2 macrophages compared with high-salt diet–treated *EP4*$^{fl/fl}$ mice. ***$P < 0.001$. $n = 4$. Original magnification, ×400. All values are shown as mean ± SEM. All P values were calculated by Student's t test.

blood was sampled to determine chimerism by determination of *Cox2* expression with PCR.

BP measurement. BP was measured in awake, chronically catheterized mice except for studies depicted in Figure 1, which utilized a tail-cuff microphonic manometer (71). For tail-cuff measurements, mice were trained for 3 consecutive days at room temperature (Monday to Wednesday) before SBP was recorded on the following 2 days (Thursday and Friday) using a tail-cuff monitor (BP-2000 BP Analysis System, Visitech Systems). SBPs recorded over 2 days were averaged and used as SBP from 1 mouse. For catheterization BP measurements, BP was recorded every minute for 1 hour, and the average of all recorded BPs was used as BP from 1 mouse. Our preliminary data indicated that BP measured by tail-cuff microphonic manometer and carotid catheterization was comparable in *Cox2*$^{-/-}$-WT and WT-WT mice on a normal-salt diet (Supplemental Figure 11). BP measurement using carotid catheterization was performed through Vanderbilt Mouse Metabolic Phenotyping Centers. Mice were anesthetized with 80 mg/kg of ketamine (Fort Dodge Laboratories) and 8 mg/kg of inactin (Byk Gulden) by i.p. injection and were placed on a temperature-controlled pad. After tracheostomy, phycoerythrin 10 tubing was inserted into the right carotid artery. The catheter was tunneled under the skin, exteriorized, secured at the back of the neck, filled with heparinized saline, and sealed. The catheterized mouse was housed individually, and 24 hours later, BP was determined with a Blood Pressure Analyzer (Micro-Med). In addition, in a subset of mice, BPs were monitored by radiotelemetry. Mice were anesthetized with nembutal (50 mg/kg, i.p.). Radiotelemetric catheters (PA-C10, Data Sciences International) were inserted into the left common carotid artery with the transmitter implanted s.c. Mice were housed individually. After 14 days, mice had recovered from

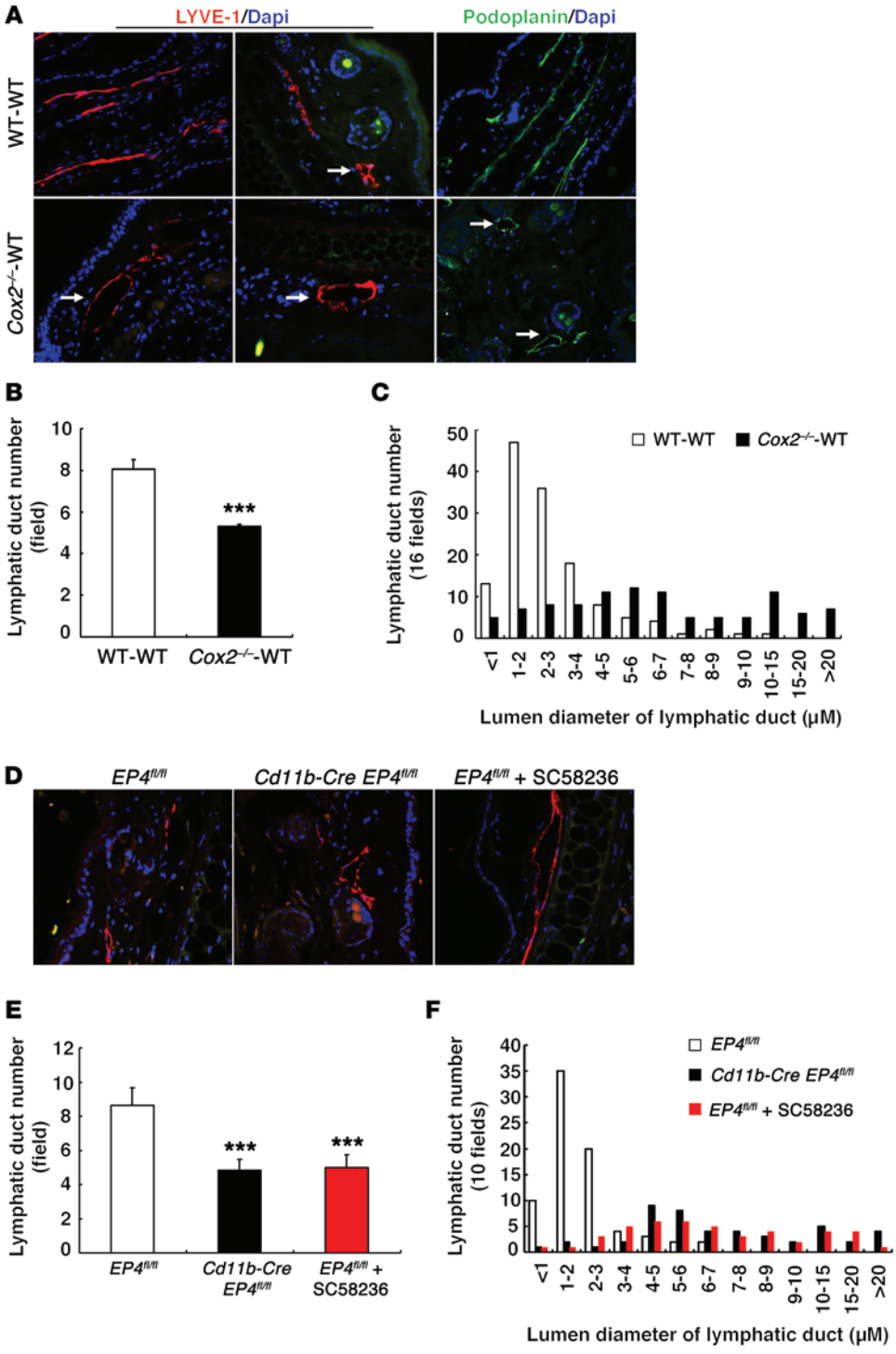

Figure 13. Mice with a deficient hematopoietic cell COX-2 pathway had abnormal skin lymphatic ducts in response to high-salt intake. (**A**) Ear lymphatic ducts were dilated in high-salt diet–treated *Cox2*$^{-/-}$-WT BMT mice, as indicated by immunostaining of LYVE-1 and podoplanin, 2 lymphatic markers. Arrows indicate lymphatic vessels. Original magnification: ×400. (**B** and **C**) High-salt–treated *Cox2*$^{-/-}$-WT BMT mice had decreased numbers of lymphatic ducts, but more dilated ducts compared with high-salt diet–treated WT-WT BMT mice. ***$P < 0.001$. $n = 4$. (**D**–**F**) Both high-salt diet–treated *Cd11b-Cre EP4*$^{fl/fl}$ and high-salt diet plus SC58236–treated *EP4*$^{fl/fl}$ mice also had reduced numbers, but more dilated lymphatic ducts compared with high-salt diet–treated *EP4*$^{fl/fl}$ mice. ***$P < 0.001$. $n = 4$. All values are shown as mean ± SEM. All P values were calculated by Student's t test.

surgery, and heart rate and BP were recorded for the duration of the study. The data from the telemetric device were collected using the Dataquest ART system, version 4.0 (Data Sciences International) by way of a RPC-1 receiver placed under the mouse cage (72).

Sodium and water balance studies with acute salt loading. Mice were housed individually to acclimate in metabolic cages for 3 days on a normal-salt diet with free access to tap water, and then a single dose of 1 mEq of NaCl was given by gavage. Urine was collected every 12 hours for 72 hours for urine volume and Na excretion. Urinary sodium excretion was determined using a flame photometer.

Measurement of tail lymphatic flow. Measurement of lymphatic flow was carried out according to a previous report, with modifications (73). Briefly, mice were anesthetized with s.c. injection of a solution containing xylazine hydrochloride (1 mg/kg, Sigma-Aldrich) and ketamine hydrochloride (10 mg/kg, Butler Animal Health Supply) and kept on a heating pad with the tail fixed. One microliter of 25% FITC-dextran (average molecular weight: 2,000 kDa, catalog 52471, Sigma-Aldrich) was injected intradermally at the tip of the tail using a microsyringe (Hamilton). The caudal-to-rostral lymphatic flow in the tail was monitored using a Nikon AZ100M microscope with fluores-

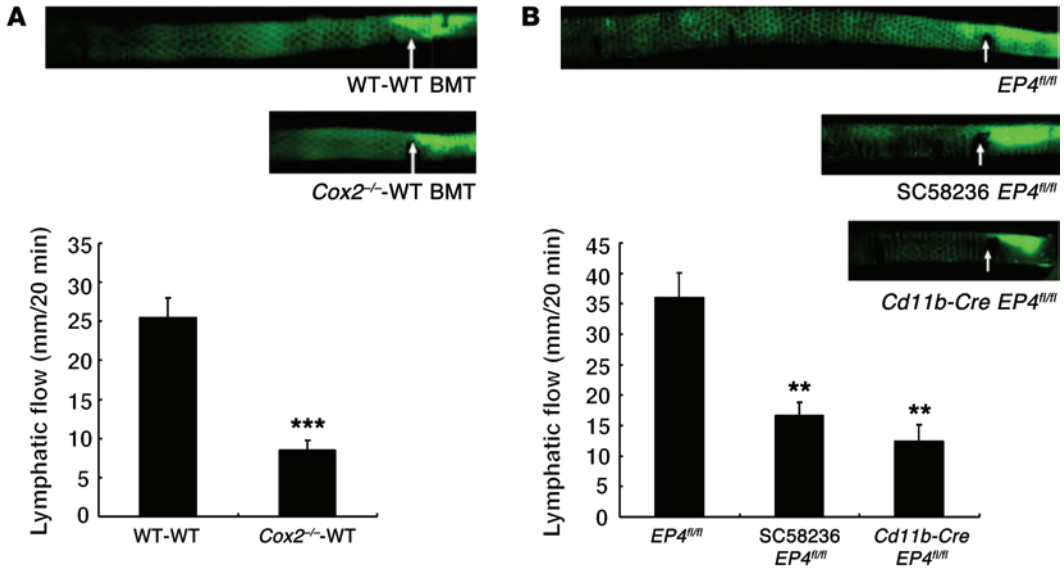

Figure 14. Mice with a deficient hematopoietic cell COX-2 pathway had impaired lymphatic flow. Mouse tails were injected with 1 μl FITC-labeled dextran, and lymphatic flow was measured. Representative experiments are indicated above, and the summary of studies in 4 separate mice in each group is indicated below. (**A**) Tail lymphatic flow was markedly slower in high-salt diet–treated *Cox2*$^{-/-}$-WT BMT mice than in high-salt diet–treated WT-WT BMT mice. ***$P < 0.001$. (**B**) Tail lymphatic flow was also significantly slower in high-salt diet–treated *Cd11b-Cre EP4*$^{fl/fl}$ mice and high-salt diet plus SC58236–treated mice. **$P < 0.01$ vs. high-salt diet–treated *EP4*$^{fl/fl}$ mice. All values are shown as mean ± SEM. All *P* values were calculated by Student's *t* test.

cent imaging mode (Vanderbilt Image Core) at ×2 magnification with time lapse for 20 minutes. The lymphatic flow rate was expressed as mm/20 minutes.

Cell culture. Murine macrophage RAW 264.7 cells purchased from ATCC were grown in DMEM supplemented with 4,500 mg/l glucose, 2 mM L-glutamine, 10% FBS, 100 U/ml penicillin, and 100 μg/ml streptomycin in 5% CO_2 and 95% air at 37°C. The cells were starved for 16 hours in medium containing 0.5% FBS, then treated for an additional 3 hours with vehicle (DMSO), EP_4 receptor antagonist, L-161,982 (20 μM dissolved in DMSO, Cayman Chemical), 10 μM PGE_2, or PGE_2 plus L-161,982, which was added 30 minutes before PGE_2. The cells were harvested for quantitative PCR (qPCR) measurements.

Polarization of RAW 264.7 cells. For ex vivo polarization of RAW 264.7 cells, M0 phenotype was achieved by culturing RAW 264.7 cells in DMEM for 48 hours, M1 phenotype by culturing RAW 264.7 cells in medium containing 1 μg/ml LPS for 24 hours, and M2 phenotype by culturing RAW 264.7 cells in medium containing IL-4 and IL-13 (10 ng/ml for each) for 48 hours (24).

Isolation of kidney and peritoneal monocytes/macrophages/dendritic cells. CD11b-expressing cells in kidney single-cell suspensions or cells isolated from the peritoneal cavity were enriched using mouse CD11b Microbeads and MACS.

Measurement of skin Na and K content. Skin Na and K content were measured by Galbraith Laboratories Inc.

Antibodies. Rabbit anti-murine COX-2 (160106) was purchased from Cayman Chemical; rat anti-mouse F4/80 (MCA497R), Ly-6G (MCA2387), CD3 (MCA1477), and CD8α (MCA2694) were purchased from AbD Serotec; rabbit anti–TNF-α (ab6671) was from R&D Systems; FOXP3 (NB100-39002) was from Novus Biologicals; rabbit anti-iNOS (ab3523) and MR (CD206, ab64693) were from Abcam; goat VEGF-C (sc-1881) and podoplanin (sc-23564), rat anti-lymphatic vessel endothelial hyaluronan receptor 1 (LYVE-1) (sc-80170), and mouse anti-SGK1 (sc28338) were from Santa Cruz Biotechnology Inc. Sheep anti–p-NCC (at Thr45, Thr50, and Thr55) was obtained from Hillary McLauchlan/James Hastie (University of Dundee, Dundee, United Kingdom).

RNA isolation and qRT-PCR. Total RNA from tissues and cultured cells was isolated using TRIzol reagents (Invitrogen). Quantitative reverse-transcriptase PCR (qRT-PCR) was performed using TaqMan real-time PCR (7900HT, Applied Biosystems). The Master Mix and all gene probes were also purchased from Applied Biosystems. The probes used in the experiments included mouse S18 (Mm02601778), *Cox2* (Mm00478374), *Cox1* (Mm00477214), *mPGES-1* (Mm00452105), *Inos* (Mm00440502), *Ccl3* (Mm00441258), arginase-1 (Mm00475991), MR (Mm01329362), *Tgfb* (Mm00441726), *Ym1* (Mm00657889), *Tnfa* (Mm99999068), *Il1a* (Mm00439621), *Il1b* (Mm00434228), *Vegfc* (Mm00437313), podoplanin (Mm00494716), *Nfat5* (Mm00467257), *EP1* (Mm00443097), *EP2* (Mm00436051), *EP3* (Mm01316856), *EP4* (Mm00436053), *Il6* (Mm00446190), *ENaCa* (Mm00803386), *ENaCb* (Mm00441215), *ENaCg* (Mm00441228), and *NCC* (Mm00490213).

Immunofluorescence/immunohistochemistry staining and quantitative image analysis. The animals were anesthetized with Nembutal (70 mg/kg, i.p.) and given heparin (1,000 units/kg, i.p.) to minimize coagulation. One kidney was removed for immunoblotting and qRT-PCR, and the animal was perfused with FPAS (3.7% formaldehyde, 10 mM sodium *m*-periodate, 40 mM phosphate buffer, and 1% acetic acid) through the aortic trunk cannulated by means of the left ventricle. The fixed kidney and skin were dehydrated through a graded series of ethanols, embedded in paraffin, sectioned (4 μm), and mounted on glass slides. Immunostaining was carried out as in previous reports (74). For both immunofluorescent and immunohistochemical staining of p-NCC, antigen retrieval was achieved by boiling in citric acid buffer (100 mM, pH 6.0) for 3 × 5 minutes. For F4/80 immunofluorescent staining, antigen retrieval was achieved by incubating in trypsin solu-

tion for 15 minutes (T-7186, Sigma-Aldrich). For double-immunofluorescent staining of F4/80 with COX-2, MR, or VEGF-C, deparaffinized sections were blocked with 10% normal goat serum plus 2% BSA for 1 hour and then incubated with rat anti-F4/80 antibodies overnight at 4°C. After washing with PBS, the section was incubated with anti-rat biotinylated IgG for 1 hour, washed with PBS, and then incubated with FITC-streptavidin. After thorough washing with PBS, the section was incubated with second primary antibodies (rabbit anti–COX-2, anti–VEGF-C, or anti-MR) for 1.5 hours at room temperature, washed with PBS, and then incubated with Cy3 anti-rabbit IgG. VECTASHIELD mounting medium with DAPI was used for nuclear staining (H-1200, Vector Laboratories). Sections were viewed and imaged with a Nikon TE300 fluorescence microscope and SPOT-cam digital camera (Diagnostic Instruments). On the basis of the distinctive density and color of immunostaining in video images, the number, size, and position of stained area were quantified by using the BIOQUANT True-Color Windows System (R & M Biometrics). Four representative fields from each animal were quantified at ×160 magnification, and their average was used as data from 1 animal sample.

Immunoblotting. Cultured cells were lysed and kidneys were homogenized with buffer containing 10 mM Tris-HCl (pH 7.4), 50 mM NaCl, 2 mM EGTA, 2 mM EDTA, 0.5% Nonidet P-40, 0.1% SDS, 100 μM Na_3VO_4, 100 mM NaF, 0.5% sodium deoxycholate, 10 mM sodium pyrophosphate, 1 mM PMSF, 10 μg/ml aprotinin, and 10 μg/ml leupeptin. The homogenate was centrifuged at 15,000 *g* for 20 minutes at 4°C. An aliquot of supernatant was taken for protein measurement with a BCA protein assay kit (ThermoScientific). Immunoblotting was as described in a recent report (75).

Flow cytometry. Mouse blood (0.5 ml) was incubated with 10 ml red blood cell lysis buffer for 10 minutes at room temperature and passed through a 50-μm mesh (Falcon; BD Biosciences), yielding single-cell suspensions. Cells were centrifuged (800 *g*, 10 min, 8°C), resuspended in FACS buffer, kept on ice, and counted. The obtained cells were incubated in 2.5 μg/ml Fc blocking solution, centrifuged again (800 × *g*, 10 min, 8°C), and resuspended with FACS buffer. 10^6 cells were stained for 20 minutes at room temperature with FITC rat anti-mouse CD45 and PE/Cy7 anti-mouse F4/80 and then washed and resuspended in FACS buffer. After immunostaining, cells were analyzed immediately on a FACSCanto II cytomer with DIVA software (BD), and off-line list mode data analysis was performed using Winlist software from Verity Software House.

Measurement of eicosanoids. Culture medium eicosanoid profiling was measured by gas chromatographic/negative ion chemical ionization mass spectrometric assays using stable isotope dilution, as described previously (76).

Statistics. All values are presented as means, with error bars representing ± SEM. Student's *t* test, ANOVA, and Bonferroni's *t* tests were used for statistical analysis.

Study approval. All animal studies were approved by the Institutional Animal Care and Use Committee of Vanderbilt University.

Author contributions

MZZ and RCH designed the studies; MZZ, BY, YW, SY, SW, and XF performed the studies; MZZ and RCH reviewed the results; MZZ and RCH wrote the manuscript.

Acknowledgments

We would like to thank Jens Titze and David Harrison for helpful discussions (Vanderbilt University), Jean Vacher for provision of CD11b-Cre mice (Clinical Research Institute of Montreal, Montreal, Quebec, Canada), and the Vanderbilt Clinical/Translational Research Center for help in telemetry measurements. This work was supported by funds from the Department of Veterans Affairs (to R.C. Harris) and NIH grants CA122620, DK38226, DK62794, and DK95785. R.C. Harris and Ming-Zhi Zhang receive NIH–National Institute of Diabetes and Digestive and Kidney Diseases funding.

Address correspondence to: Raymond C. Harris, Division of Nephrology, C3121 MCN, Vanderbilt University School of Medicine, and Nashville Veterans Affairs Hospital, Nashville, Tennessee 37232, USA. Phone: 615.322.2150; E-mail: ray.harris@vanderbilt.edu. Or to: Ming-Zhi Zhang, S-3206 MCN, Vanderbilt University Medical Center, Nashville, Tennessee 37232, USA. Phone: 615.343.1548; Fax: 615.343.2675; E-mail: ming-zhi.zhang@vanderbilt.edu.

1. Kanbay M, Chen Y, Solak Y, Sanders PW. Mechanisms and consequences of salt sensitivity and dietary salt intake. *Curr Opin Nephrol Hypertens*. 2011;20(1):37–43.
2. Whorton A, et al. Prostaglandins and renin release. I. Stimulation of renin release from rabbit renal cortical slices by PGI2. *Prostaglandins*. 1977;14(6):1095–1104.
3. Francisco LJ, Osborn JL, DiBona GF. Prostaglandins in renin release during sodium deprivation. *Am J Physiol*. 1982;243(6):F537–F542.
4. Linas SL. Role of prostaglandins in renin secretion in the isolated kidney. *AmJ Physiol*. 1984;246(6 pt 2):F811–F818.
5. Ito S, Carretero OA, Abe K, Juncos LA, Yoshinaga K. Macula densa control of renin release and glomerular hemodynamics. *Tohoku J Exp Med*. 1992;166(1):27–39.
6. Ito S, Carretero OA, Abe K, Beierwaltes WH, Yoshinaga K. Effect of prostanoids on renin release from rabbit afferent arterioles with and without macula densa. *Kidney Int*. 1989;35(5):1138–1144.
7. Greenberg SG, Lorenz JN, He XR, Schnermann JB, Briggs JP. Effect of prostaglandin synthesis inhibition on macula densa-stimulated renin secretion. *Am J Physiol*. 1993;265(4 pt 2):F578–F583.
8. Needleman P, Turk J, Jakschik BA, Morrison AR, Lefkowith JB. Arachidonic acid metabolism. *Annu Rev Biochem*. 1986;55:69–102.
9. Cheng HF, Harris RC. Renal effects of nonsteroidal anti-inflammatory drugs and selective cyclooxygenase-2 inhibitors. *Curr Pharm Des*. 2005;11(14):1795–1804.
10. Svendsen KB, Bech JN, Sorensen TB, Pedersen EB. A comparison of the effects of etodolac and ibuprofen on renal haemodynamics, tubular function, renin, vasopressin and urinary excretion of albumin and alpha-glutathione-S-transferase in healthy subjects: a placebo-controlled cross-over study. *Eur J Clin Pharmacol*. 2000;56(5):383–388.
11. Whelton A, Hamilton CW. Nonsteroidal anti-inflammatory drugs: effects on kidney function. *J Clin Pharmacol*. 1991;31(7):588–598.
12. Kohsaka S, et al. Increased risk of incident stroke associated with the cyclooxygenase 2 (COX-2) G-765C polymorphism in African-Americans: the Atherosclerosis Risk in Communities Study. *Atherosclerosis*. 2008;196(2):926–930.
13. Hernanz R, Briones AM, Salaices M, Alonso MJ. New roles for old pathways? A circuitous relationship between reactive oxygen species and cyclo-oxygenase in hypertension. *Clin Sci (Lond)*. 2014;126(2):111–121.
14. Yu Y, et al. Vascular COX-2 modulates blood pressure and thrombosis in mice. *Sci Transl Med*. 2012;4(132):132ra54.
15. Harrison DG, Marvar PJ, Titze JM. Vascular inflammatory cells in hypertension. *Front Physiol*.

2012;3:128.
16. Guzik TJ, et al. Role of the T cell in the genesis of angiotensin II induced hypertension and vascular dysfunction. *J Exp Med*. 2007;204(10):2449–2460.
17. Johnson RJ, Lanaspa MA, Gabriela Sánchez-Lozada L, Rodriguez-Iturbe B. The discovery of hypertension: evolving views on the role of the kidneys, and current hot topics. *Am J Physiol Renal Physiol*. 2015;308(3):F167–F178.
18. Titze J, et al. Osmotically inactive skin Na^+ storage in rats. *Am J Physiol Renal Physiol*. 2003;285(6):F1108–F1117.
19. Machnik A, et al. Macrophages regulate salt-dependent volume and blood pressure by a vascular endothelial growth factor-C-dependent buffering mechanism. *Nat Med*. 2009;15(5):545–552.
20. Machnik A, et al. Mononuclear phagocyte system depletion blocks interstitial tonicity-responsive enhancer binding protein/vascular endothelial growth factor C expression and induces salt-sensitive hypertension in rats. *Hypertension*. 2010;55(3):755–761.
21. Karnezis T, Shayan R, Fox S, Achen MG, Stacker SA. The connection between lymphangiogenic signalling and prostaglandin biology: a missing link in the metastatic pathway. *Oncotarget*. 2012;3(8):893–906.
22. Komhoff M, et al. Cyclooxygenase-2-selective inhibitors impair glomerulogenesis and renal cortical development. *Kidney Int*. 2000;57(2):414–422.
23. Yang T, Huang YG, Ye W, Hansen P, Schnermann JB, Briggs JP. Influence of genetic background and gender on hypertension and renal failure in COX-2-deficient mice. *Am J Physiol Renal Physiol*. 2005;288(6):F1125–F1132.
24. Zhang M-Z, et al. CSF-1 signaling mediates recovery from acute kidney injury. *J Clin Invest*. 2012;122(12):4519–4532.
25. Hara S, Kamei D, Sasaki Y, Tanemoto A, Nakatani Y, Murakami M. Prostaglandin E synthases: understanding their pathophysiological roles through mouse genetic models. *Biochimie*. 2010;92(6):651–659.
26. Nataraj C, et al. Receptors for prostaglandin E(2) that regulate cellular immune responses in the mouse. *J Clin Invest*. 2001;108(8):1229–1235.
27. Richardson C, et al. Activation of the thiazide-sensitive Na^+-Cl^- cotransporter by the WNK-regulated kinases SPAK and OSR1. *J Cell Sci*. 2008;121(pt 5):675–684.
28. Kopp C, et al. 23Na magnetic resonance imaging-determined tissue sodium in healthy subjects and hypertensive patients. *Hypertension*. 2013;61(3):635–640.
29. Kleinewietfeld M, et al. Sodium chloride drives autoimmune disease by the induction of pathogenic TH17 cells. *Nature*. 2013;496(7446):518–522.
30. Wu C, et al. Induction of pathogenic TH17 cells by inducible salt-sensing kinase SGK1. *Nature*. 2013;496(7446):513–517.
31. Hagendoorn J, et al. Endothelial nitric oxide synthase regulates microlymphatic flow via collecting lymphatics. *Circ Res*. 2004;95(2):204–209.
32. Kashiwagi S, Hosono K, Suzuki T, Takeda A, Uchinuma E, Majima M. Role of COX-2 in lymphangiogenesis and restoration of lymphatic flow in secondary lymphedema. *Lab Invest*. 2011;91(9):1314–1325.
33. Johnson AG, Nguyen TV, Day RO. Do nonsteroidal anti-inflammatory drugs affect blood pressure? A meta-analysis. *Ann Intern Med*. 1994;121(4):289–300.
34. Harris RC, McKanna JA, Akai Y, Jacobson HR, Dubois RN, Breyer MD. Cyclooxygenase-2 is associated with the macula densa of rat kidney and increases with salt restriction. *J Clin Invest*. 1994;94(6):2504–2510.
35. Yang T, et al. Regulation of cyclooxygenase expression in the kidney by dietary salt intake. *Am J Physiol*. 1998;274(3 pt 2):F481–F489.
36. Catella-Lawson F, et al. Effects of specific inhibition of cyclooxygenase-2 on sodium balance, hemodynamics, and vasoactive eicosanoids. *J Pharmacol Exp Ther*. 1999;289(2):735–741.
37. Rodriguez F, Llinas MT, Gonzalez JD, Rivera J, Salazar FJ. Renal changes induced by a cyclooxygenase-2 inhibitor during normal and low sodium intake. *Hypertension*. 2000;36(2):276–281.
38. Qi Z, et al. Opposite effects of cyclooxygenase-1 and -2 activity on the pressor response to angiotensin II. *J Clin Invest*. 2002;110(1):61–69.
39. Yao B, Harris RC, Zhang MZ. Interactions between 11beta-hydroxysteroid dehydrogenase and COX-2 in kidney. *Am J Physiol Regul Integr Comp Physiol*. 2005;288(6):R1767–R1773.
40. Zewde T, Mattson DL. Inhibition of cyclooxygenase-2 in the rat renal medulla leads to sodium-sensitive hypertension. *Hypertension*. 2004;44(4):424–428.
41. Sasaki Y, et al. Microsomal prostaglandin E synthase-1 is involved in multiple steps of colon carcinogenesis. *Oncogene*. 2012;31(24):2943–2952.
42. Eruslanov E, Daurkin I, Ortiz J, Vieweg J, Kusmartsev S. Pivotal advance: tumor-mediated induction of myeloid-derived suppressor cells and M2-polarized macrophages by altering intracellular PGE(2) catabolism in myeloid cells. *J Leukoc Biol*. 2010;88(5):839–848.
43. Takayama K, Garcia-Cardena G, Sukhova GK, Comander J, Gimbrone MA Jr, Libby P. Prostaglandin E2 suppresses chemokine production in human macrophages through the EP4 receptor. *J Biol Chem*. 2002;277(46):44147–44154.
44. Rodriguez-Iturbe B, Pons H, Quiroz Y, Johnson RJ. The immunological basis of hypertension. *Am J Hypertens*. 2014;27(11):1327–1337.
45. Wenzel P, et al. Lysozyme M-positive monocytes mediate angiotensin II-induced arterial hypertension and vascular dysfunction. *Circulation*. 2011;124(12):1370–1381.
46. Elmarakby AA, et al. Chemokine receptor 2b inhibition provides renal protection in angiotensin II - salt hypertension. *Hypertension*. 2007;50(6):1069–1076.
47. Chan CT, et al. Reversal of vascular macrophage accumulation and hypertension by a CCR2 antagonist in deoxycorticosterone/salt-treated mice. *Hypertension*. 2012;60(5):1207–1212.
48. Pires PW, Girgla SS, McClain JL, Kaminski NE, van Rooijen N, Dorrance AM. Improvement in middle cerebral artery structure and endothelial function in stroke-prone spontaneously hypertensive rats after macrophage depletion. *Microcirculation*. 2013;20(7):650–661.
49. Zandbergen HR, et al. Macrophage depletion in hypertensive rats accelerates development of cardiomyopathy. *J Cardiovasc Pharmacol Ther*. 2009;14(1):68–75.
50. De Miguel C, Rudemiller NP, Abais JM, Mattson DL. Inflammation and hypertension: new understandings and potential therapeutic targets. *Curr Hypertens Rep*. 2015;17(1):507.
51. Kirabo A, et al. DC isoketal-modified proteins activate T cells and promote hypertension. *J Clin Invest*. 2014;124(10):4642–4656.
52. Chen L, Zhu Y, Zhang G, Gao C, Zhong W, Zhang X. CD83-stimulated monocytes suppress T-cell immune responses through production of prostaglandin E2. *Proc Natl Acad Sci U S A*. 2011;108(46):18778–18783.
53. Goetzl EJ, An S, Zeng L. Specific suppression by prostaglandin E2 of activation-induced apoptosis of human $CD4^+CD8^+$ T lymphoblasts. *J Immunol*. 1995;154(3):1041–1047.
54. Ahmadi M, Emery DC, Morgan DJ. Prevention of both direct and cross-priming of antitumor $CD8^+$ T-cell responses following overproduction of prostaglandin E2 by tumor cells in vivo. *Cancer Res*. 2008;68(18):7520–7529.
55. Pablos JL, Santiago B, Carreira PE, Galindo M, Gomez-Reino JJ. Cyclooxygenase-1 and -2 are expressed by human T cells. *Clin Exp Immunol*. 1999;115(1):86–90.
56. Ryan EP, Pollock SJ, Murant TI, Bernstein SH, Felgar RE, Phipps RP. Activated human B lymphocytes express cyclooxygenase-2 and cyclooxygenase inhibitors attenuate antibody production. *J Immunol*. 2005;174(5):2619–2626.
57. Subramanya AR, Ellison DH. Distal convoluted tubule. *Clin J Am Soc Nephrol*. 2014;9(12):2147–2163.
58. Kamat NV, et al. Renal transporter activation during angiotensin-II hypertension is blunted in interferon-$\gamma^{-/-}$ and interleukin-$17A^{-/-}$ mice. *Hypertension*. 2015;65(3):569–576.
59. Nguyen MT, Lee DH, Delpire E, McDonough AA. Differential regulation of Na^+ transporters along nephron during ANG II-dependent hypertension: distal stimulation counteracted by proximal inhibition. *Am J Physiol Renal Physiol*. 2013;305(4):F510–F519.
60. Jia Z, Aoyagi T, Kohan DE, Yang T. mPGES-1 deletion impairs aldosterone escape and enhances sodium appetite. *Am J Physiol Renal Physiol*. 2010;299(1):F155–F166.
61. Wiig H, et al. Immune cells control skin lymphatic electrolyte homeostasis and blood pressure. *J Clin Invest*. 2013;123(7):2803–2815.
62. Su JL, et al. Cyclooxygenase-2 induces EP1- and HER-2/Neu-dependent vascular endothelial growth factor-C up-regulation: a novel mechanism of lymphangiogenesis in lung adenocarcinoma. *Cancer Res*. 2004;64(2):554–564.
63. Timoshenko AV, Chakraborty C, Wagner GF, Lala PK. COX-2-mediated stimulation of the lymphangiogenic factor VEGF-C in human breast cancer. *Br J Cancer*. 2006;94(8):1154–1163.
64. Iwata C, et al. Inhibition of cyclooxygenase-2 suppresses lymph node metastasis via reduction of lymphangiogenesis. *Cancer Res*. 2007;67(21):10181–10189.
65. Hosono K, et al. Roles of prostaglandin E2-EP3/EP4 receptor signaling in the enhancement of

lymphangiogenesis during fibroblast growth factor-2-induced granulation formation. *Arterioscler Thromb Vasc Biol*. 2011;31(5):1049–1058.
66. Kashiwagi S, Hosono K, Suzuki T, Takeda A, Uchinuma E, Majima M. Role of COX-2 in lymphangiogenesis and restoration of lymphatic flow in secondary lymphedema. *Lab Invest*. 2011;91(9):1314–1325.
67. Dinchuk JE, et al. Renal abnormalities and an altered inflammatory response in mice lacking cyclooxygenase II. *Nature*. 1995;378(6555):406–409.
68. Schneider A, et al. Generation of a conditional allele of the mouse prostaglandin EP4 receptor. *Genesis*. 2004;40(1):7–14.
69. Ferron M, Vacher J. Targeted expression of Cre recombinase in macrophages and osteoclasts in transgenic mice. *Genesis*. 2005;41(3):138–145.
70. Nishida M, et al. Absence of angiotensin II type 1 receptor in bone marrow-derived cells is detrimental in the evolution of renal fibrosis. *J Clin Invest*. 2002;110(12):1859–1868.
71. Yao B, Harris RC, Zhang MZ. Intrarenal dopamine attenuates deoxycorticosterone acetate/high salt-induced blood pressure elevation in part through activation of a medullary cyclooxygenase 2 pathway. *Hypertension*. 2009;54(5):1077–1083.
72. Zhang MZ, et al. Intrarenal dopamine deficiency leads to hypertension and decreased longevity in mice. *J Clin Invest*. 2011;121(7):2845–2854.
73. Leu AJ, Berk DA, Yuan F, Jain RK. Flow velocity in the superficial lymphatic network of the mouse tail. *Am J Physiol*. 1994;267(4 pt 2):H1507–H1513.
74. Zhang MZ, Yao B, Cheng HF, Wang SW, Inagami T, Harris RC. Renal cortical cyclooxygenase 2 expression is differentially regulated by angiotensin II AT(1) and AT(2) receptors. *Proc Natl Acad Sci U S A*. 2006;103(43):16045–16050.
75. Zhang MZ, et al. Role of epoxyeicosatrienoic acids (EETs) in mediation of dopamine's effects in the kidney. *Am J Physiol Renal Physiol*. 2013;305(12):F1680–F1686.
76. Zhang MZ, et al. Inhibition of 11beta-hydroxysteroid dehydrogenase type II selectively blocks the tumor COX-2 pathway and suppresses colon carcinogenesis in mice and humans. *J Clin Invest*. 2009;119(4):876–885.